World Academy of Science, Engineering and Technology
International Journal of Electronics and Communication Engineering
Vol:18, No:2, 2024

Design and Optimization of Coplanar Waveguide-Fed Sensing Antennas for ISM Band Applications

Vivek Bharti, Inderpreet Kaur, Saurabh Verma, Renu Gangwar, Hari Kumar Singh

Abstract—This work presents a dual-band Coplanar Waveguide (CPW) fed rectangular patch antenna designed for applications in Industrial, Scientific, and Medical (ISM) Band sensing. Fabricated on a cost-effective FR-4 substrate with specific dimensions, the antenna incorporates a rectangular slot and a copper patch, optimized through simulation to achieve desired characteristics, particularly focusing on the reflection coefficient. A unique feature is introduced through the integration of copper cells forming a Partially Reflecting Surface (PRS) to feed the antenna. Dual-band functionality is achieved, covering frequencies of 1.28 GHz-1.3 GHz and 4.9 GHz-5.2 GHz, catering to diverse communication needs within these frequency ranges. The addition of a superstrate enhances the antenna's gain, resulting in 4.5 dBi at 1.28 GHz-1.3 GHz and 6.5 dBi at 4.9 GHz-5.2 GHz, with an efficiency of 58%.

Keywords—ISM, Coplanar waveguide fed, superstrate, circularly polarized.

I. Introduction

THE rapid expansion of digitization has led to a proliferation of radio frequency (RF) signal emitters. With an increasing number of devices engaged in communication, there is a corresponding rise in ambient RF signals in the environment. Due to the ubiquity of RF waves, a relatively new communication technique called ambient backscatter communications (AmBC) has gained prominence in the last decade. This method has heightened awareness of ambient radiofrequency energy utilization [1]. However, achieving optimal design for the antenna, which is critical to the AmBC system, remains challenging. Bao and colleagues [2] proposed the use of a single-band omnidirectional antenna, while Muhammad et al. [3] suggested a dual-band antenna for gathering radio frequency energy from the surrounding environment. Among various feeding methods, CPW slot antennas fed by CPW have garnered increased attention. The CPW feed is often seen as an alternative to microstrip line feed due to its advantages, such as compatibility, ease of construction, and wideband properties. These advantages are realized through the utilization of microwave-integrated circuits, particularly monolithic microwave integrated circuits (MMIC), and active components [4].

Numerous designs have been explored in academic literature, with studies employing various techniques on CPW-fed structures to attain circular polarization across a broad spectrum [5]–[11]. In [5] the cross-patch engraved in the middle of a square slot supplied by CPW revealed the circular polarization. In [6], a T-shaped structure positioned at the side of the slot incorporated a single strip attached to it, showcasing an identical CP characteristic. Nevertheless, [7] and [8] introduced perturbations to the two opposite corners of square holes to generate circularly polarized (CP) radiation. Additionally, in [9], a proposed antenna attained a broad CP bandwidth by connecting the center of a CPW signal strip within a square hole featuring a check-shaped strip with a 45° rotation. In reference [10], the structure included two grounded inverted-L engravings. Reference [11] depicted a circular slot. This approach involved expanding a CPW strip to incorporate an inverted L shape. Subsequently, to achieve broadband operation, two grounded inverted-L strips were introduced within the circular opening. However, the axial ratio bandwidth (ARBW) in each of the aforementioned experiments is not sufficiently broad to encompass ubiquitous radio frequencies.

In proposed work, we recommend a printed CPW-fed CP slot antenna with broadband performance. It is capable of operating in various communication standards such as 3G, 4G, LTE, GSM 1800/1900, the 2.4GHz band, and 2100/2300/2500 Wi-Fi channels. This antenna design provides a 3-dB axial ratio bandwidth (ARBW) ranging from 2.681 GHz to 1.747 GHz. The technique applied stimulates the antenna to produce circularly polarized radiation within a planar, single-layer structure.

A. Antenna Designing

The design of the CPW-fed slot antenna is illustrated in Fig. 1, with specific dimensions detailed in Table I. Fabricated on an affordable single-sided FR-4 substrate featuring a relative permittivity of 4.4, a loss tangent of 0.015, and a thickness of 1.6 mm, the substrate adopts a square shape with a side length of L, resulting in overall dimensions of 120×120×1.6 mm^3. A rectangular slot, measuring 65 mm in length and 33 mm in width, is carved from the top layer. A copper rectangular patch is then inserted into the slot, while two identical gaps are introduced with a spacing of g = 0.47 mm between the ground plane and the CPW strip.

The analysis and design process involved initial simulations using software. Subsequent optimization led to determining the antenna dimensions, influenced by parameters such as the reflection coefficient and the dimensions of the rectangular slot. Certain parameters, like the substrate size, were approximated during this process. To facilitate feeding

Hari Kumar Singh is with Department Of Electronics and Communication, Mahatma Jyotiba Phule Rohilkhand University Bareilly, India (corresponding author, e-mail: hari.singh@mjpru.ac.in).

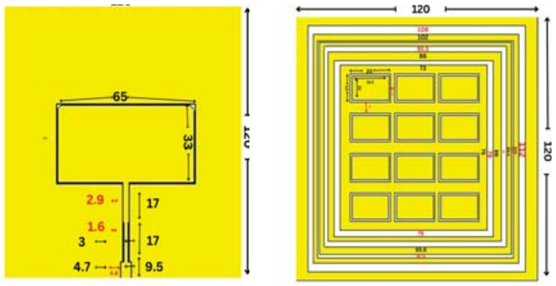

(a) (b)

Fig. 1 (a) First layer Top, (b) Superstrate Top

the antenna, copper cells were integrated to form a PRS, as depicted in Fig. 1 (b). Each unit cell consists of a rectangular loop with dimensions of 65×33 mm². The optimal antenna parameters are provided in Table I.

TABLE I
DESIGN PARAMETER (DP) AND ITS CALCULATED VALUE (CV) FOR THE ANTENNA

DP	CV (mm)	DP	CV (mm)
L	120	B	120
$fw1$	2.9	$fw2$	1.6
$fw3$	4.7	$fl1$	17
$fl2$	17	$fl3$	9.3
$Rl1$	65	$Rb1$	33

TABLE II
DESIGN PARAMETER (DP) AND ITS CALCULATED VALUE (CV) FOR THE SUPERSTRATE

DP	CV(mm)	DP	CV(mm)	DP	CV(mm)	DP	CV(mm)
$Sl1$	20	$Sl2$	13	$si1$	18.5	$si2$	11
$St1$	108	$st2$	102	$st3$	90.5	$St4$	86
$st5$	73	$su1$	112	$Su2$	104	$su3$	96.4
$su4$	81	$Su5$	86	$su6$	79	$su7$	75

II. RESULT & DISCUSSION

A. Scattering Parameters

The parameter to consider is the width of the director. The outcomes exhibit variability, revealing that it exerts minimal influence on both the low and high-frequency bands. However, it plays a crucial role in determining the antenna's gain, specifically directing it toward the z-direction at higher operating frequencies. In contrast, g2 explicitly impacts the performance in the high-frequency band.

B. Parametric Studies

A variety of parameters have been systematically adjusted to assess the characteristics of the proposed antenna. The initial parameter under consideration is the gap between the substrate and the superstrate, and the corresponding reflection coefficient results for different gap values are depicted in Fig. 2. Notably, the gap is observed to have a discernible impact on the gain, wherein an increase in the gap leads to a noticeable effect. The second parameter, denoted as ”w” for the width of the patch, is explored, and Fig. 3 presents the

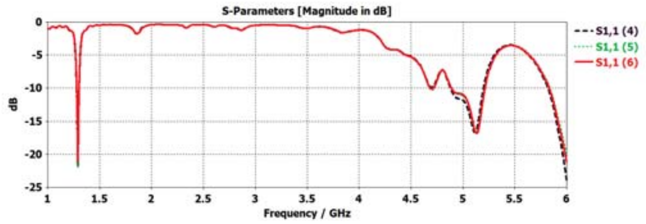

(a)

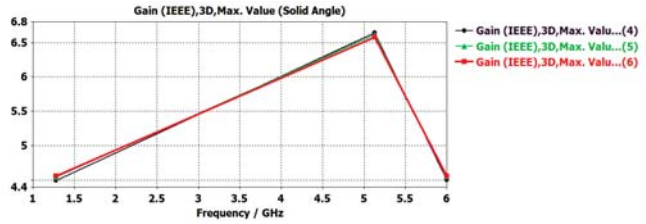

(b)

Fig. 2 Variation in the gap between substrate and superstrate: (a) Reflection coefficient, (b) gain

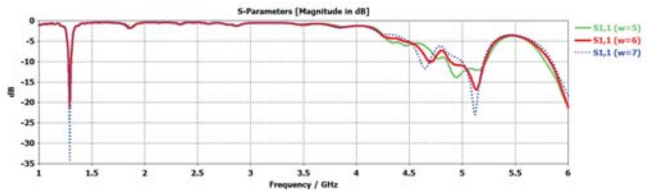

(a)

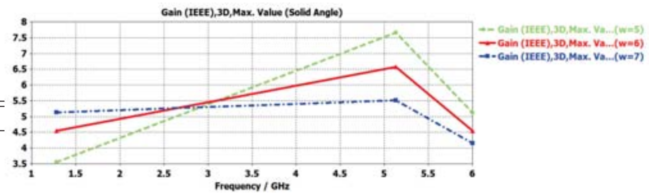

(b)

Fig. 3 Variation of the width of the Patch: (a) Reflection coefficient, (b) gain

results of this variation. Interestingly, it is observed that ”w” has minimal influence on the low-frequency band. However, as ”w” increases from 64.5 mm to 65.0 mm and 65.5 mm, there is an increase in the impedance of the low-frequency band. The third parameter, represented as ”L” for the length of the patch, is examined, and Fig. 5 illustrates the reflection coefficient results for different ”L” values. It becomes evident that ”L” is particularly influential in the high-frequency band (5.15–5.85 GHz), especially concerning the low-resonant mode. An increase in ”L” from 32.5 mm to 33 mm and 33.5 mm results in a significant elevation of the low-resonant mode, leading to a decrease in bandwidth.

C. Surface Current Distribution

The CST software was employed to simulate the surface current distribution of the proposed CPW-fed antenna. In Fig. 5, the current distribution on the surface is illustrated at 1.28 GHz, 5.13 GHz, and 6 GHz, revealing a uniform flow of current across the antenna surface. The magnitude of

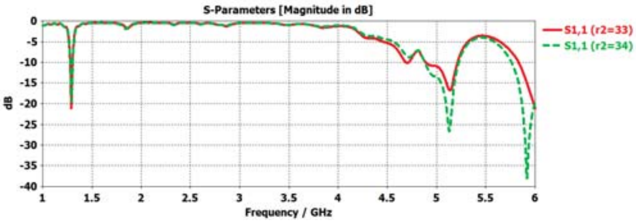

(a)

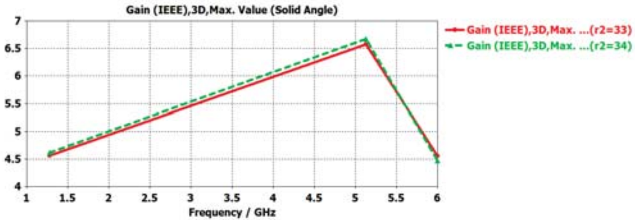

(b)

Fig. 4 Variation of the L of the Patch: (a) Reflection coefficient, (b) gain

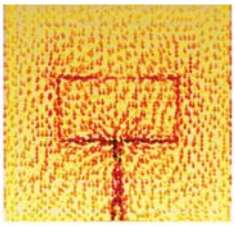

(a)

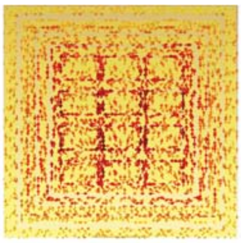

(b)

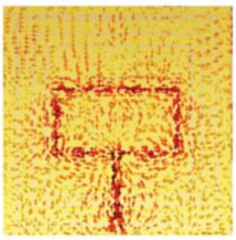

(c)

(d)

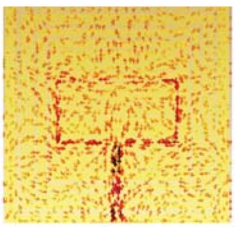

(e)

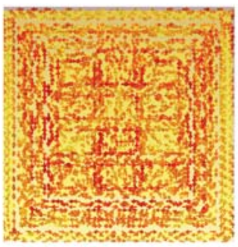

(f)

Fig. 5 Surface Current At 1.28 GHz: (a) rectangular patch, (b) Superstrate At 5.13 GHz, (c) rectangular patch, (d) Superstrate At 6 GHz, (e) rectangular patch, (f) Superstrate

the current distribution was examined at these frequencies.at 1.28 GHz, as shown in Figs.5 (a) & (b), the current is uniformly distributed over the entire antenna surface. This uniform distribution confirms that, at this frequency, the antenna effectively radiates energy into the surrounding space. At 5.13 GHz, as depicted in Figs. 5 (c) & (d), the surface current is notably concentrated over the resonating stub. This concentration indicates that the energy is primarily stored in the resonator rather than being radiated into the surrounding air. In contrast, at 6 GHz, as shown in Figs. 5 (e) & (f), the current is uniformly distributed over the entire antenna surface. This uniform distribution confirms that, at this frequency, the antenna effectively radiates energy into the surrounding space.

D. Radiation Pattern

The operational frequencies observed are 1.28 GHz, 5.13 GHz, and 6 GHz, as illustrated in Fig. 6. Figs. 6 (a) & (b) present a comparison between the normalized simulated H-plane and E-plane co-polarization patterns at 1.28 GHz 78.3 degrees and 62.2 degrees. Figs. 6 (c)& (d) present normalized simulated xz-plane and yz-plane co-polarization patterns at 5.13 GHz 26.9 degrees and 19.1 degrees. Figs. 6 (e) & (f) present normalized simulated xz-plane and yz-plane co-polarization patterns at 6 GHz 38.5 degrees and 27.3 degrees.

E. Far Field Performance

Figs. 7 and 8 depict the efficiency, gain, and 3D Polar plot of the proposed structure. The efficiency is 58% at 1.28 GHz and 55% at 5.13 GHz gain increases from 4.5 GHz to 6.5 GHz from low-frequency band to high-frequency band. The radiation pattern is highly directive.

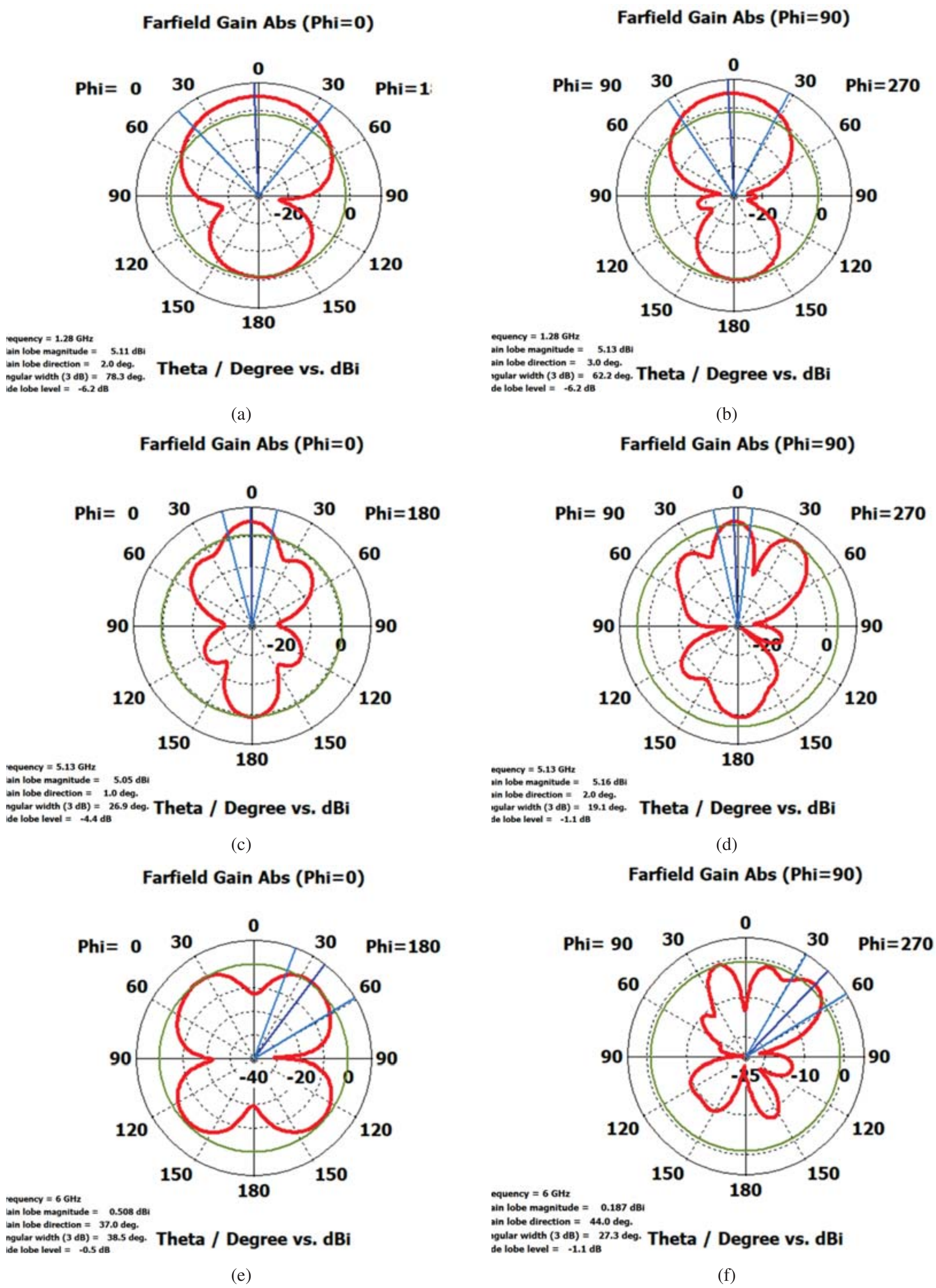

Fig. 6 At 1.28 Ghz: (a) phi = 0 degree, (b) phi = 90 degree; at 5.13 GHz: (c) phi = 0 degree, (d) phi = 90 degree; at 6 GHz: (e) phi = 0 degree, (f) phi = 90 degree

III. Conclusion

A compact broadband CPW-fed rectangular patch antenna was proposed for harvesting ambient RF signals. The Rectangular patch is connected to the CPW transition strip, to enhance the impedance bandwidth. The superstrate is employed to enhance the gain obtained results showed that the antenna is matched from 1.28 GHz to 1.3 GHz, and 4.8GHz to 5.2 GHz, covering common wireless bands such as GSM 1800/1900, 3G/4G/LTE 2100/2300/2500. Hence, the suggested antenna is well-suited for energy harvesting across diverse wireless communication bands.

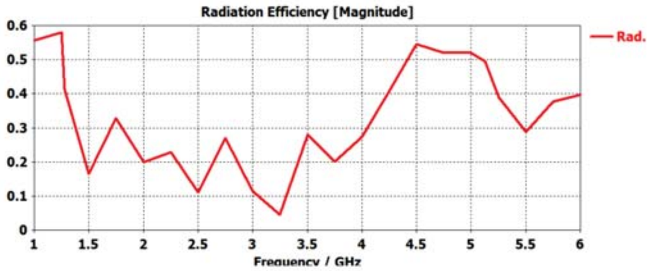

(a)

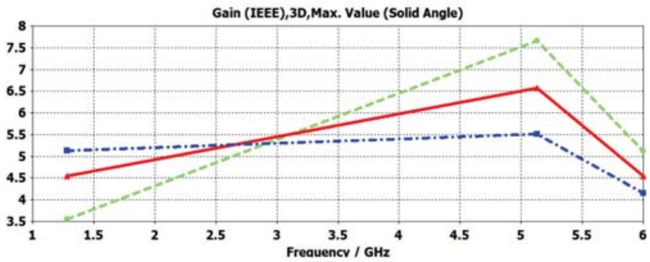

(b)

Fig. 7 (a) Efficiency, (b) Gain

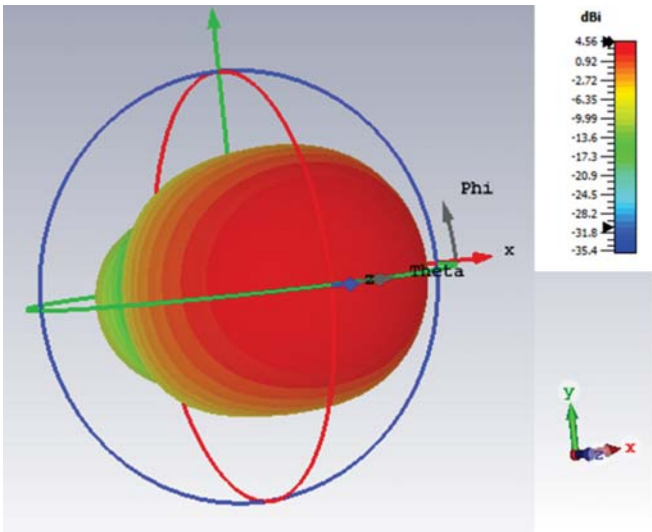

Fig. 8 3D Polar plot

References

[1] Liu, A. Parks, V. Talla, S. Gollakota, D. Wetherall, and J. R. Smith, "Ambient backscatter: Wireless communication out of thin air," ACM SIGCOMM Computer Communication Review, vol. 43, pp., 39–50, Aug. 2013.

[2] X. Bao, K. Yang, O. O'Conchubhair, and M. J. Ammann, "Differentially-fed omnidirectional circularly polarized patch antenna for RF energy harvesting," in 2016 10th European Conference on Antennas and Propagation (EuCAP), pp. 1–5, Apr. 2016.

[3] S. Muhammad, J. J. Tiang, S. K. Wong, A. Smida, R. Ghayoula, and A. Iqbal, "A dual-band ambient energy harvesting rectenna design for wireless power communications," IEEE Access, vol. 9, pp. 99944–99953, Jul. 2021.

[4] K.-L. Wong, Compact and broadband microstrip antennas, vol. 168. John Wiley & Sons, Apr. 2004.

[5] C. Chou, K. Lin, and H. Su, "Broadband circularly polarised cross patch-loaded square slot antenna," Electronics Letters, vol. 43, pp. 485–486, Apr. 2007.

[6] J.-Y. Sze, K.-L. Wong, and C.-C. Huang, "Coplanar waveguide-fed square slot antenna for broadband circularly polarized radiation," IEEE Transactions on Antennas and Propagation, vol. 51, pp. 2141–2144, Aug. 2003.

[7] Y.-Y. Chen, Y.-C. Jiao, G. Zhao, W. Zhang, and H.-H. Xie, "A novel compact slot antenna for broadband circularly polarized radiation," in Proceedings of the 9th International Symposium on Antennas, Propagation and EM Theory, pp. 201–204, Dec. 2010.

[8] P. M. Paul, K. Kandasamy, and M. S. Sharawi, "A corner expanded CPW-fed slot antenna with circular polarization characteristics," in 2019 13th European Conference on Antennas and Propagation (EuCAP), pp. 1–3, Jun. 2019.

[9] Y. Liu and P. Hsu, "Broadband circularly polarised square slot antenna fed by coplanar waveguide," Electronics letters, vol. 49, pp. 976–977, Aug. 2013.

[10] J.-Y. Sze and C.-C. Chang, "Circularly polarized square slot antenna with a pair of inverted-L grounded strips," IEEE Antennas and Wireless Propagation Letters, vol. 7, pp. 149–151, Mar. 2008.

[11] R. Orr, G. Goussetis, and V. Fusco, "Design method for circularly polarized Fabry-P´erot cavity antennas," IEEE Transactions on Antennas and Propagation, vol. 62, no. 1, pp. 19–26, 2013.